

# Push-Pull Direct CAD Modeling with Movable Neighboring Faces for Preserving $G^1$ Connections

Qiang Zou, Hsi-Yung Feng\*

Department of Mechanical Engineering

The University of British Columbia

Vancouver, BC

Canada V6T 1Z4

## Abstract

B-rep model editing plays an essential role in CAD and motivates the very recent direct modeling CAD paradigm, which features intuitive push-pull manipulation of the model geometry. Boundary faces in a B-rep model could be connected in a smooth manner, typically  $G^1$  continuous, for functional, manufacturing or aesthetic reasons. Quite often, it is desirable to preserve such smooth connections during push-pull moves. This is however no trivial matter and introduces additional challenges. To preserve the  $G^1$  connections, neighboring faces of push-pulled faces need to be made movable, but their motions are not known explicitly. Consequently, it becomes challenging to track the geometry-topology inconsistency caused by these movable faces and to attain a robust update for push-pulled solid models. No effective ways exist in the literature to deal with the challenges; the industrial state of the art has implemented this function, but the challenges are not addressed satisfactorily and robustness issues are observed. This paper proposes a novel reverse tracking method to solve the above challenges, and then, based on it, presents a systematic method for push-pull direct modeling while preserving  $G^1$  connections. The developed method has been validated with a series of case studies.

*Keywords:* Computer-aided design; Direct modeling;  $G^1$  connections; Topology changes

## 1. Introduction

Boundary representation (B-rep) models are fundamental to computer-aided design (CAD). Particularly, almost all export/import 3D CAD models are B-rep solid models made in the STEP/IGES formats [1]. Interactive environments for editing such models thus play an important part in CAD systems. These environments require intuitive, flexible model manipulation and fast model update. The very recent direct modeling CAD paradigm encompasses all these characteristics. In direct modeling, the primary feature/function is the intuitive push-pull interactions with the geometry (boundary faces) of the model [2,3]. Such push-pull controls allow models to be modified very easily, and ultimately leading to faster iterations between design alternatives and simulations.

Push-pull direct modeling allows the user to effectively reshape a solid model through pushing/pulling (i.e., moving) its boundary faces. On the other hand, a moved boundary face may cause changes made to the connections between this boundary face and its neighboring boundary faces. If the changes are intended exactly by the user or the changed connections are trivial, this way of working is more than adequate. Nevertheless, there are also many scenarios in which these boundary faces are connected in a smooth manner for considerations like stress concentration reduction, manufacturability, injury prevention (from sharp edges), or even aesthetic design [4], which make the connections non-trivial. Because of these design intents, the user may want the smooth connections to be preserved during push-pull edits. It is thus necessary for direct modelers to provide the option of push-pull direct modeling while preserving the smooth connections.

The smooth connections stated above can be  $G^1$  or higher.  $G^1$  is the first order geometric continuity and states that two boundary faces share common normal direction along their joint edge (or equivalently, they are connected tangentially) [5]. Smooth connections of a higher order than  $G^1$  are also seen in B-rep models but only in models involving free-form surfaces. This work focuses on models composed of linear and quadratic surfaces, and such models cover about 95% of models in mechanical design according to [6]. In this regard, the problem in this work is

---

\* Corresponding author. Tel.: +1-604-822-1366; fax: +1-604-822-2403.  
E-mail: john.qiangzou@gmail.com (Q. Zou), feng@mech.ubc.ca (H.-Y. Feng)

to be stated as: push-pull direct modeling of featureless B-rep solid models while preserving the involved  $G^1$  continuous connections (shortly push-pull with  $G^1$  connections).

Push-pull with  $G^1$  connections is no trivial matter. The core task to implement push-pull direct modeling is to handle the geometry-topology inconsistency caused by the movable boundary faces [7,8]. Two types of movable boundary faces exist in push-pull with  $G^1$  connections: the boundary faces pushed-pulled by the user and the neighboring boundary faces driven by the pushed-pulled boundary faces (in order to keep the  $G^1$  connections). The second type of driven boundary faces is new to push-pull direct modeling and leads to additional challenges. The driven boundary faces move according to how the user moves the pushed-pulled boundary faces, but the motions of the driven boundary faces are not quite known in fact. That is, the driven boundary faces' motions are governed by a system of tangent constraints representing the  $G^1$  connections; not until this system is solved do we know the positions/orientations of the driven boundary faces for any intermediate instants during the push-pull edit. There are thus no explicit expressions for the driven boundary faces' motions. One may obtain an approximation to the motions through a brute-force sampling/solving, but the resulting high computational load makes this strategy unattractive. As a result, the lack of the driven boundary faces' motions clearly makes it challenging to track the geometry-topology inconsistency. On the other hand, tracking the geometry-topology inconsistency is the basis for a robust handling of the geometry-topology inconsistency [7,8].

The challenges stated above cannot be effectively handled by the existing methods in the literature because their methods of tracking geometry-topology inconsistency are heuristic-based and the necessary condition for applying those heuristics is to know beforehand the motions of all movable boundary faces. The solutions provided by industry are not satisfactory either: push-pull with  $G^1$  connections is either partially supported for a few selected scenarios or fully supported but with robustness issues. This work presents a systematic, robust method for push-pull with  $G^1$  connections. It solves the above challenges through a novel reverse inference method, which features an effective tracking of the geometry-topology inconsistency while avoiding the reliance on the motion information of movable boundary faces.

## 2. Related work

The notion of push-pull direct modeling was initially proposed by industry to meet the increasing need for efficient and flexible model editing capability in reuse of existing designs [9]. Due to the practical significance of push-pull with  $G^1$  connections, it has been implemented in a few commercial CAD systems. However, the implementation information is often kept private or patented, as it may lead to competitive advantages for CAD vendors. As a result, none of the CAD systems comes with guarantees or with clearly stated limitations. In fact, robust issues are observed for push-pull with  $G^1$  connections in these CAD systems: they work well in some situations but not in others. In some CAD systems, push-pull with  $G^1$  connections is not even fully supported. For example, Autodesk Inventor (2018) is only able to preserve the  $G^1$  connections relating with fillets. In this regard, the current solutions provided by industry are far from being complete.

The direct modeling notion is relatively new in CAD, and thus there is a limited amount of published research literature about push-pull direct modeling methodologies. Among the published work related to push-pull direct modeling [7,8,10–13], no effective ways exist to deal with the challenges stated previously for push-pull with  $G^1$  connections. Lipp et al. [7] restricted the models undergoing push-pull edits to solid polygonal meshes that are essentially composed only of planar faces. For such models, there are no  $G^1$  connections between boundary faces. Zou and Feng [8] proposed a continuity-based method for push-pulling solid models composed of linear and quadratic surfaces, but no particular attention was given to  $G^1$  connections. In both methods, heuristics were employed to track the geometry-topology inconsistency during push-pull edits. While these heuristics are effective for the original problems, they are not applicable to the problem in this work. This is because knowing beforehand the motions of all movable boundary faces is a necessary condition for the heuristics to work properly, but this is not the case for push-pull with  $G^1$  connections. There are also studies [10–13] approaching push-pull direct modeling from the perspective of feature-based modeling [14]. These methods essentially translate push-pull edits to parametric feature edits. Such a strategy is clearly not suitable for handling the featureless B-rep solid models as in this work.

The persistent naming problem in feature-based CAD is related but not directly connected to the present work. A major task in this topic is to compute the parameter range within which the model topology remains unchanged [15]. The limits of this parameter range are the critical points at which the model topology changes. The notion of these critical points is (conceptually) related to the geometry-topology inconsistency tracking in this work. However, the methods presented in [15–17] are not suitable for this work due to the reliance on the parametric relationships in the model, which is not available in featureless B-rep models.

### 3. Methodology

For better presenting the proposed method, several important notions to be used in the following text are made precise first. Every push-pull edit is followed by a regeneration of the boundary representation for the push-pulled model, which is referred to as model regeneration. The regeneration is essentially a boundary evaluation based on the post-edit carrier surfaces and the pre-edit topology [18] (see Fig. 1 for a trivial example). The aforementioned geometry-topology inconsistency refers to the situation in which the regenerated model is invalid (non-solid). This means that the topology presented in the regenerated model is different from the pre-edit topology, which either adds new face-face connections or lose old face-face connections. Fig. 1 shows one such example. Model update means resolving the geometry-topology inconsistency so to attain a valid modeling result.

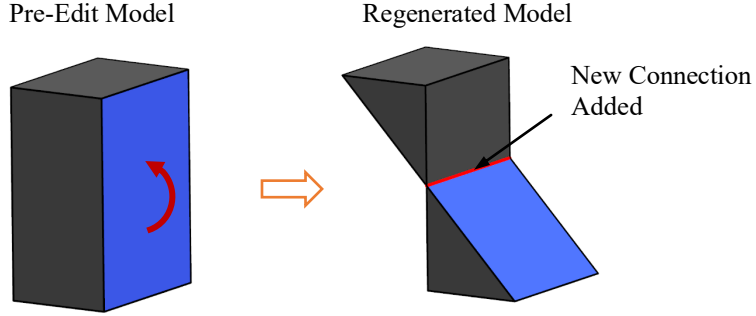


Figure 1 Example of model regeneration and geometry-topology inconsistency.

The method to be presented in this paper is outlined in Fig. 2. The part in the dash rectangle represents the main body of the method, which iteratively applies two procedures: geometry-topology inconsistency detection and resolution. The geometry-topology inconsistency detection means evaluating the next critical point at which the geometry-topology inconsistency occurs. The geometry-topology inconsistency resolution is to resolve the geometry-topology inconsistency immediately after it is detected. The resulting model will serve as the base model in the next iteration for carrying out the rest part of the push-pull edit. These two procedures are repeated until no critical point is to be detected. Then, model regeneration gives the intended model for the whole push-pull edit.

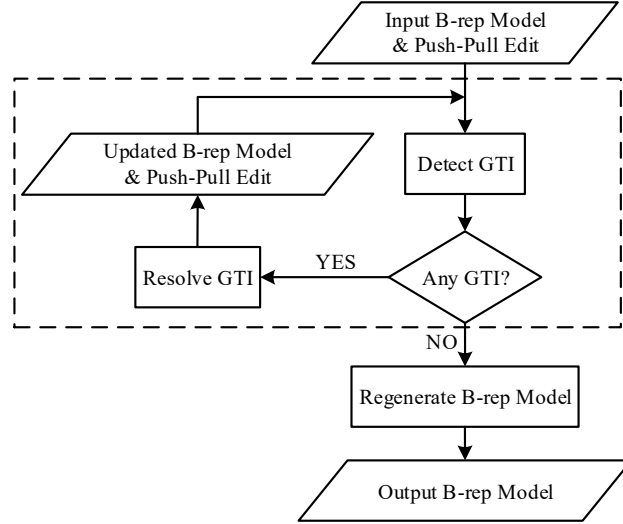


Figure 2 Schematic diagram of the overall method (GTI: geometry-topology inconsistency).

The above iterative strategy allows each geometry-topology inconsistency emerging in a push-pull edit to be handled individually and avoids any possible coupling among the inconsistencies. This strategy is not new in fact, and has been used in the previous work [7,8]. Nevertheless, this strategy is easy to state but challenging to realize. The previous methods/ideas [7,8,16,17] related to geometry-topology inconsistency detection are essentially prediction-

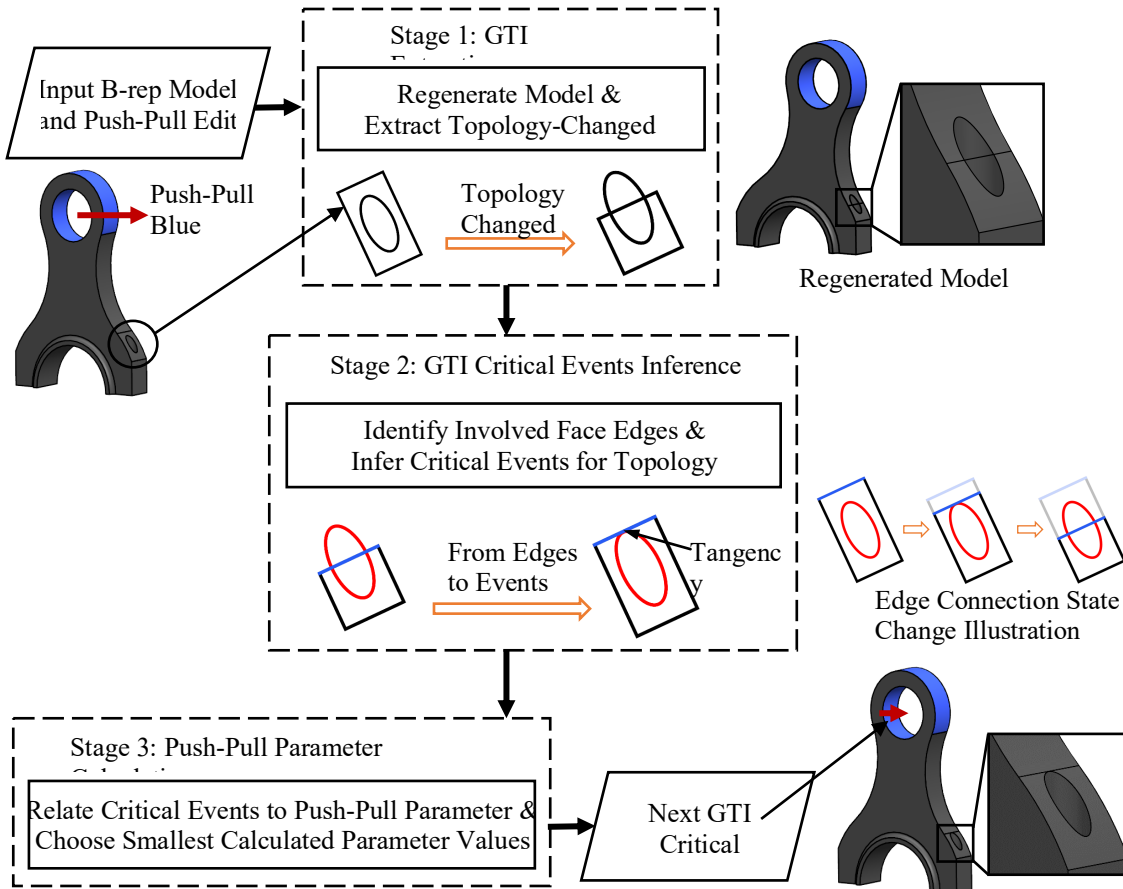


Figure 3 Workflow of geometry-topology inconsistency detection (GTI: geometry-topology inconsistency).

based, which recognizes pre-set geometry-topology inconsistency patterns during face moving. A general, exhaustive checking without considering the special characteristics of the specific model and push-pull edit will involve much unnecessary checking, making it very inefficient. To make matters much worse, knowing the motions of movable boundary faces is a necessary condition for the successful application of these methods; however, this is not the case for push-pull with  $G^1$  connections, as discussed in Section 1.

Without an effective method for geometry-topology inconsistency detection, the above iterative strategy cannot be made possible. In this regard, a novel detection approach is to be proposed, which can avoid the exhaustive checking and reliance on the motion information of movable boundary faces. The basic idea is to investigate the geometry-topology inconsistencies presented in the regenerated model, and then to reversely trace back to the critical points where these inconsistencies occur. This idea is radically different from the previous work, and comprises the main contribution of the present work. In terms of the second procedure of geometry-topology inconsistency resolution, the methods developed in [7,8] are still applicable since push-pull with  $G^1$  connections do not introduce additional inconsistency types. Thus, this work uses a similar method to carry out the inconsistency resolution.

### 3.1. Geometry-Topology Inconsistency Detection

To implement the reverse inference idea stated above, the detection module is made up of three consecutive stages, as illustrated in Fig. 3. An example based on a connecting rod part is also given to assist the understanding of the workflow. In Stage 1, a model regeneration is first performed. If there are no geometry-topology inconsistencies in the regenerated model (i.e., a valid model is output), nothing further needs to be done. If otherwise, we extract the newly added connections and/or lost connections. Such connection changes are reflected in the changes made to the edge topology on the boundary faces, as connections essentially define intersections between carrier surfaces (see the circled face in Fig. 3 for an example) [8]. Thus, the extraction is simply done by collecting the topology-changed boundary faces in the regenerated model.

In Stage 2, we first identify the subjects of the topology changes on each topology-changed boundary face. That is, the edges involved in the topology changes are identified, as exemplified by the blue and red edges in Fig. 3. With these edges in place, we then analyze how their connection states change, i.e., how two edges change from being apart to being connected, or the other way around. This analysis serves as a basis for reversely inferring critical events where edge connection states alter abruptly. For example, the event for the blue and red edges in Fig. 3 is the tangency between them. Inferring such events is straightforward using human intuition, but not the case with a computer. In the following, an effective method will be presented to handle this challenge.

In Stage 3, each of the critical events attained from Stage 2 is related to the push-pull parameter (the translation distance and/or rotation angle) through a system of nonlinear equations. Let the push-pull parameter be represented by  $t \in [0,1]$ . By solving the system for each critical event, we attain a new set  $\{t_i\}_{i=1}^n$  collecting all the critical points at which the critical events occur. The smallest element in this set is then the intended result of geometry-topology inconsistency detection.

Among the above three stages, the essential parts are clearly the reverse inferring from topology-changed boundary faces to critical events and the relating of these events to the push-pull parameter. Novel methods are to be presented to deal with them in the rest part of this section.

### 3.1.1. Reverse Inferring of Critical Events

Without loss of generality, we focus on one topology-changed boundary face. This face is from the regenerated model, and thus referred to as the regenerated face. Its corresponding face in the pre-edit model is called the reference face. Recall that the very first task in the reverse inference is to attain the edges involved in the topology changes, which gives rise to the need of retrieving and manipulating the topological information of a boundary face. To facilitate such processing, a graph-based face representation scheme is used: connections of edges on a face are represented by a graph structure in which nodes encode the edge entities on the face and arcs describe the connections between the edges entities. Fig. 4 shows an example of this graph representation scheme, using the reference and regenerated faces of the connecting rod example in Fig. 3.

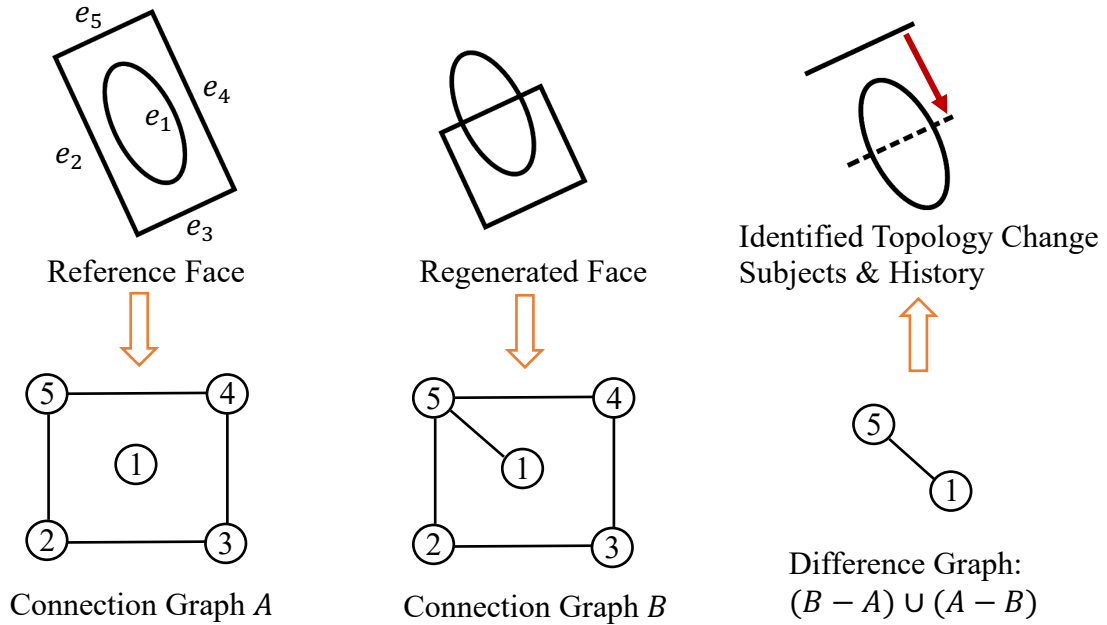


Figure 4 Graph representation of boundary faces and identification of topology change subjects and history.

One advantage of the graph representation is the many operators available for manipulating graphs. Those of interest are the Boolean operations that can extract the difference between two graphs. More specifically, the difference between the connection graphs of the reference and regenerated faces  $G_{ref}, G_{reg}$  is given by:

$$\Delta G = (G_{reg} - G_{ref}) \cup (G_{ref} - G_{reg}) \quad (1)$$

The first subtraction acquires the newly added connections in  $G_{reg}$  (w.r.t.  $G_{ref}$ ), and the second subtraction attains the lost connections in  $G_{reg}$  (w.r.t.  $G_{ref}$ ). Their union then gives the difference of the connections. It should be noted that Boolean operations on graphs have various definitions [19]. Here, an edge-based definition is used. To be more specific, let two graphs be  $G_1 = (V_1, E_1)$  and  $G_2 = (V_2, E_2)$ , where  $V_1$  or  $2$  is the node set and  $E_1$  or  $2$  the arc set. Graph subtraction is then given as  $G_1 - G_2 = (\{\text{nodes induced from } E_1 - E_2\}, E_1 - E_2)$ , and the same for graph union. For example, applying Eq. 1 to the two connection graphs in Fig. 4 yields a difference graph that correctly captures the newly added connection between edges  $e_1$  and  $e_5$ .

The difference graph in Eq. 1 not only tells the subjects of topology changes but also carries part of the information of the topology changes' progression history. Given a difference graph  $\Delta G = (\Delta V, \Delta E)$ , we can easily check if an arc  $e \in \Delta E$  is from the regenerated connection graph  $G_{reg}$  or the reference connection graph  $G_{ref}$ . If  $e$  is from  $G_{reg}$ , it represents a newly added connection, and thus the two edges' connection state progressed from being apart to being connected. If  $e$  is from  $G_{ref}$ , it represents a lost connection, and thus the connection state progressed from being connected to being apart. Consider again the example in Fig. 4. The only arc of the difference graph comes from the connection graph  $B$  (i.e.,  $G_{reg}$ ) and the topology change is a consequence of edges  $e_1$  and  $e_5$  moving into each other, as illustrated by the red arrow.

A difference graph gives a list of edge pairs (having connection state changes) on the boundary face and their individual progression histories. Each progression thread makes either two originally disconnected edges connected, or the other way around. The critical event for the progression from disconnection to connection is the collision between the two edges. Generally, edge-edge collision has two configurations (1) involving only interior points of both edges and (2) having end points involved, as shown in Fig. 5. These two configurations have different characteristic events. As can be seen from Fig. 5, the event for the left configuration is the interior-point tangency between the two edges, and that for the right one is the end-point incidence. It should be noted here that no further information is available for us to determine which of the two critical events has actually occurred for a specific progression since we have little information on the movable boundary faces' motions. As a result, both events are possible and need to be checked. For the second progression type, i.e., from connection to disconnection, the critical



Figure 5 Example configurations of edge-edge collision.

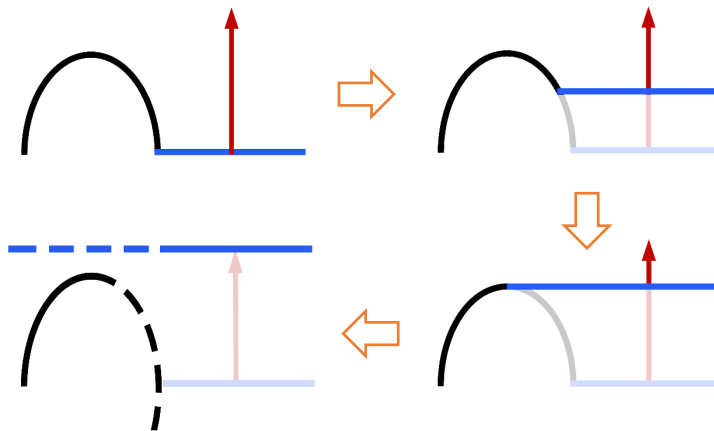


Figure 6 Example process of edge-edge separation.

event is the separation between the carrier curves of the two edges, as shown in Fig. 6. More precisely, one of the curves moved beyond the size limit of the other curve and the characteristic event is the tangency at the ends of the two edges.

### 3.1.2. Mathematical Modeling of Critical Events

With the critical events in place, we need to relate them to the push-pull parameter so to attain the critical points at which these events occur. From the previous discussion, there are three critical events: interior-point tangency, end-point incidence, and end-point tangency. They can be further reduced to the following two basic types: tangency and incidence. It will be shown in the following that these two event types are to be formulated as systems of quadratic equations.

A tangency (interior-point or end-point) between two edges can be expressed in terms of (1) the tangency between the carrier curves of the two edges and (2) the examination of the tangency locating inside the limits of the edges, in a sequential manner. More formally, let the edges be represented as  $e_1, e_2$ , their respective carrier curves be  $c_1, c_2$ , and assume that the tangency of the two curves is at point  $p$ . Then,  $p$  clearly has to satisfy the on-curve conditions:

$$p \in c_1 \text{ and } p \in c_2 \quad (2)$$

In general, carrier curves in a B-rep model are intersections of surfaces [20]. Thus, the on-curve conditions can be modeled as:

$$\begin{aligned} p \in c_1 &\Leftrightarrow \begin{cases} F_1(p) = 0 \\ F_2(p) = 0 \end{cases} \\ p \in c_2 &\Leftrightarrow \begin{cases} F_2(p) = 0 \\ F_3(p) = 0 \end{cases} \end{aligned} \quad (3)$$

where  $F_1(\cdot) = 0$ ,  $F_2(\cdot) = 0$  and  $F_3(\cdot) = 0$  denote the equations of the surfaces adjacent to carrier curves  $c_1, c_2$ , refer to Fig. 7 for an illustration of their relationship.

In addition to the on-curve conditions, point  $p$  also needs to satisfy the tangency condition that the two curves have collinear tangents at point  $p$ . The tangent for curve  $c_1$  (or  $c_2$ ) is given by the cross product of the normals of the surfaces  $F_1$  and  $F_2$  (or,  $F_2$  and  $F_3$ ). The normal of a surface  $F(x, y, z) = 0$  is given by its gradient:  $\nabla F = \left( \frac{\partial F}{\partial x}, \frac{\partial F}{\partial y}, \frac{\partial F}{\partial z} \right)$  [21]. The tangency condition can then be formulated as:

$$\begin{aligned} (\nabla F_1(p) \times \nabla F_2(p)) \times (\nabla F_2(p) \times \nabla F_3(p)) &= \mathbf{0} \\ \Leftrightarrow \nabla F_2(p) \cdot (\nabla F_1(p) \times \nabla F_3(p)) &= 0 \end{aligned} \quad (4)$$

where operators  $\times$  and  $\cdot$  denote the cross product and dot product, respectively. Combining Eq. 4 with Eq. 3 yields the mathematical modeling of the tangency event.

For an incidence event at edge ends, it should first satisfy the on-curve conditions (i.e., Eq. 3) as well, and then satisfy the additional constraint that point  $p$  is at edge ends. As shown in Fig. 7, the top end of edge  $e_1$  is the intersection of curve  $c_1$  and the surface  $F_4$ . Thus, to impose the edge end constraint, we only need to require that point  $p$  is on surface  $F_4$ , which is given by:

$$F_4(p) = 0 \quad (5)$$

This equation, together with Eq. 3, gives the mathematical modeling of the incidence event.

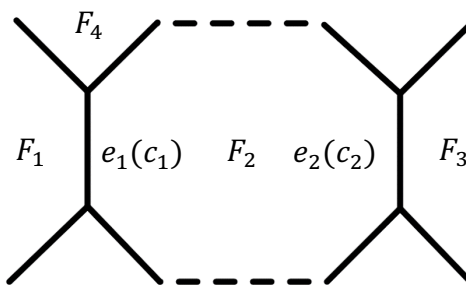


Figure 7 Illustration of edge-curve-surface relationship.

In the above formulations, there are four equations but three variables (i.e., the three coordinates of point  $p$ ) for the tangency event (Eqs. 3 and 4), and the same for the incidence event (Eqs. 3 and 5). The missing variable is reserved for the push-pull parameter. Let the push-pull edit applied by the user be represented by a rigid transformation matrix  $T(t)$ ,  $t \in [0,1]$ . This transformation matrix imposes the motion on push-pulled boundary faces, which in turn drive the neighboring boundary faces to move due to the  $G^1$  connections between them. The motions of all these boundary faces are governed by a set of tangent constraints between their carrier surfaces, which ensures that the  $G^1$  connections between the boundary faces are to be preserved during the push-pull move. These tangent constraints can be translated trivially to a system of nonlinear equations using the existing research results in geometric constraint solving such as [22]. Combining these equations with Eqs. 3 and 4 (or 5) yields a new system of nonlinear equations that relates the push-pull parameter to a critical event detected previously. In other words, by solving this new system, we can attain the exact value of the parameter at which a given critical event occurs.

Although constructing the tangent constraints and associated equations is straightforward, a practical note should be made here. One can easily imagine a push-pull edit example in which the push-pulled boundary face has  $G^1$  connections with some of its neighboring boundary faces, and these neighboring boundary faces also have  $G^1$  connections with their neighboring boundary faces, and so forth. The question then arises: which boundary faces involved in this chain of  $G^1$  connections are movable? Different selections of boundary faces lead to different systems of tangent constraints, which then yield different push-pull results. The scheme used in this work is as follows: only the push-pulled boundary faces and their immediate neighboring boundary faces are movable. This scheme is used, simply because it is the very choice of the state-of-art CAD systems like Siemens NX and ANSYS SpaceClaim. Other schemes are also possible and the method presented in this work is readily applicable.

In summary, Algorithm 1 shows how to combine the methods described previously to achieve an effective method for geometry-topology inconsistency detection. This algorithm follows the workflow in Fig. 3: first attain topology-changed boundary faces (Line 2); then collect critical events using the method described in Section 3.1.1 (Line 5); then relate the collected critical events to the push-pull parameter with the method described in Section 3.1.2 (Lines 6-9); finally set the next critical point to the smallest of the calculated critical points.

---

**Algorithm 1:** Geometry-Topology Inconsistency Detection

---

**Input:**  $M, T(t), t \in [0,1]$  – the B-rep model and push-pull edit

**Output:** the next critical point

---

1.  $M' \leftarrow \text{RegenerateModel}(M, T(t = 1))$
2.  $F \leftarrow \text{GetTopologyChangedFaces}(M')$
3.  $T' \leftarrow \emptyset$  // for storing critical points
4. **for** each face  $f \in F$  **do**
5.      $E \leftarrow \text{InferCriticalEvents}(f)$
6.     **for** each event  $e \in E$  **do**
7.          $t' \leftarrow \text{RelateEventToPushPullParameter}(e, t)$
8.         add  $t'$  to  $T'$  if  $0 \leq t' \leq 1$  // filter out invalid critical points
9.     **end for**
10. **end for**
11. **Return**  $\text{Min}(T')$

---

### 3.2. Geometry-Topology Inconsistency Resolution

From the framework in Fig. 2, the subsequent task after attaining the next critical point is to resolve the geometry-topology inconsistency generated when the push-pull edit crosses the critical point. To do so, we need to modify the topology of the boundary faces involved in the geometry-topology inconsistency so that the resulting model is valid and the model variation is continuous. These two requirements can be implemented as either a bunch of topology editing heuristics [7] or Boolean operations on the model volume [8]. (The continuous requirement was not stated explicitly in [7], but the heuristics developed yield a continuous variation on model volume.) Both strategies are applicable to the resolution problem for push-pull with  $G^1$  connections. The Boolean-based method is used in this work as this method allows an easier implementation using the existing Boolean operation functions in modern geometric modeling kernels. In the following, a conceptual description of the method is to be presented. The detailed description and associated algorithmic procedures can be found in [8].

It is mandatory that the resulting model is a solid model [10]. This requirement is made trivial as we are using Boolean operations on the model volume to carry out the inconsistency resolution and such operations ensure model validity. The second requirement of continuous model variation states that an infinitesimal change made to the push-

pull parameter yields an infinitesimal change in the resulting model [23]. Let the model variation over the push-pull edit be represented by  $M(t), t \in [0,1]$ . The requirement is then formulated as:

$$f(M(t + \varepsilon), M(t)) \rightarrow 0 \quad \text{when } \varepsilon \rightarrow 0 \quad (6)$$

where  $f(M_1, M_2)$  is a function quantifying the difference between models  $M_1$  and  $M_2$ . In this work, the model attribute of volume is used in the function  $f$ . Eq. 6 can be related to Boolean operations on the model volume using the following intuition. Consider a moved boundary face at two points  $t$  and  $t + \varepsilon$ , and assume that the model material/volume is being removed over the domain  $[t, t + \varepsilon]$ . We can subdivide the volume of model  $M(t)$  into two parts: one in between the boundary face's carrier surface at  $t$  and that at  $t + \varepsilon$  (denoting this part as  $\Delta M$ ), and the other consisting of the rest. The second part will be simply used as the model variation at  $t + \varepsilon$ . Then, we have the following relationship  $M(t + \varepsilon) = M(t) - \Delta M$ . Clearly, if  $\varepsilon \rightarrow 0$ , then  $\Delta M \rightarrow \emptyset$ , and then  $M(t + \varepsilon) \rightarrow M(t)$ . Extending the domain  $[t, t + \varepsilon]$  to a larger one from a critical point to the next and using the same equation  $M(t + \varepsilon) = M(t) - \Delta M$  lead to the Boolean-based resolution scheme.

The above statements represent a high-level description of the idea in the Boolean-based resolution method. The whole method clearly involves more technical issues like handling a moved boundary face adding material/volume to the model, and addressing interferences among model  $\Delta M$  of multiple moved boundary faces. These issues can be solved with the variations of the idea stated above and the detailed solutions can be found in [8].

### 3.3. Overall Algorithm for Push-Pull with $G^1$ Connections

With the geometry-topology inconsistency detection method (Section 3.1) and resolution method (Section 3.2) in place, an algorithm is readily available for handling any geometry-topology inconsistencies in push-pull with  $G^1$  Connections. The algorithm is essentially an implementation of the diagram in Fig. 2 and replaces the blocks of Detect GTI and Resolve GTI with the corresponding methods in Sections 3.1 and 3.2. The specific procedures of the algorithm are shown in Algorithm 2. Line 2 corresponds to the inconsistency detection method described in Section 3.1. Line 4 corresponds to the Boolean-based resolution method described in Section 3.2. Line 5 updates the B-rep model with the model resulting from the inconsistency resolution, and Line 6 updates the push-pull edit with the rest part, which is given by  $T(1) T(t')^{-1}$ . These updates (Lines 5-7) prepare the model and push-pull edit for the next iteration.

---

#### Algorithm 2: Push-Pull with $G^1$ Connections

---

**Input:**  $M, T(t), t \in [0,1]$  – the B-rep model and push-pull edit  
**Output:** the updated model

---

1. **while** *TRUE*
2.      $t' \leftarrow \text{DetectNextCriticalPoint}(M, T)$  // Algorithms 1, Section 3.1
3.     **if**  $t' \neq \text{NULL}$  **then** // *NULL* means there is no critical point
4.          $M' \leftarrow \text{ResolveInconsistency}(M, T(t'))$  // Section 3.2
5.          $M \leftarrow M'$  // update the B-rep model
6.          $T \leftarrow T(1) T(t')^{-1}$  // update the push-pull edit
7.         Reparametrize  $T$  to the domain  $[0,1]$
8.     **else** break the loop
9.     **end while**
10.     $M \leftarrow \text{RegenerateModel}(M, T(1))$
11.    **Return**  $M$

---

## 4. Implementation and Case Studies

### 4.1. Implementation

The methodology presented previously has been implemented in an Apple Macintosh environment using C++. The implementation was built on top of the open source geometric modeling kernel OpenCASCADE (7.0); the graphical user interface was designed with QT (5.7); and the internal architecture is similar to the geometry processing and rendering framework OpenFlipper [24]. When a STEP/IGES model is imported, its boundary representation is displayed in the View window and its handle is listed in the Objects toolbox (labelled as 1 in Fig. 8a). This model handle allows the user to control the model's display parameters like hide/show. To push-pull a B-rep model displayed in the View window, the user first activates the push-pull direct modeling function by pressing the left button in the

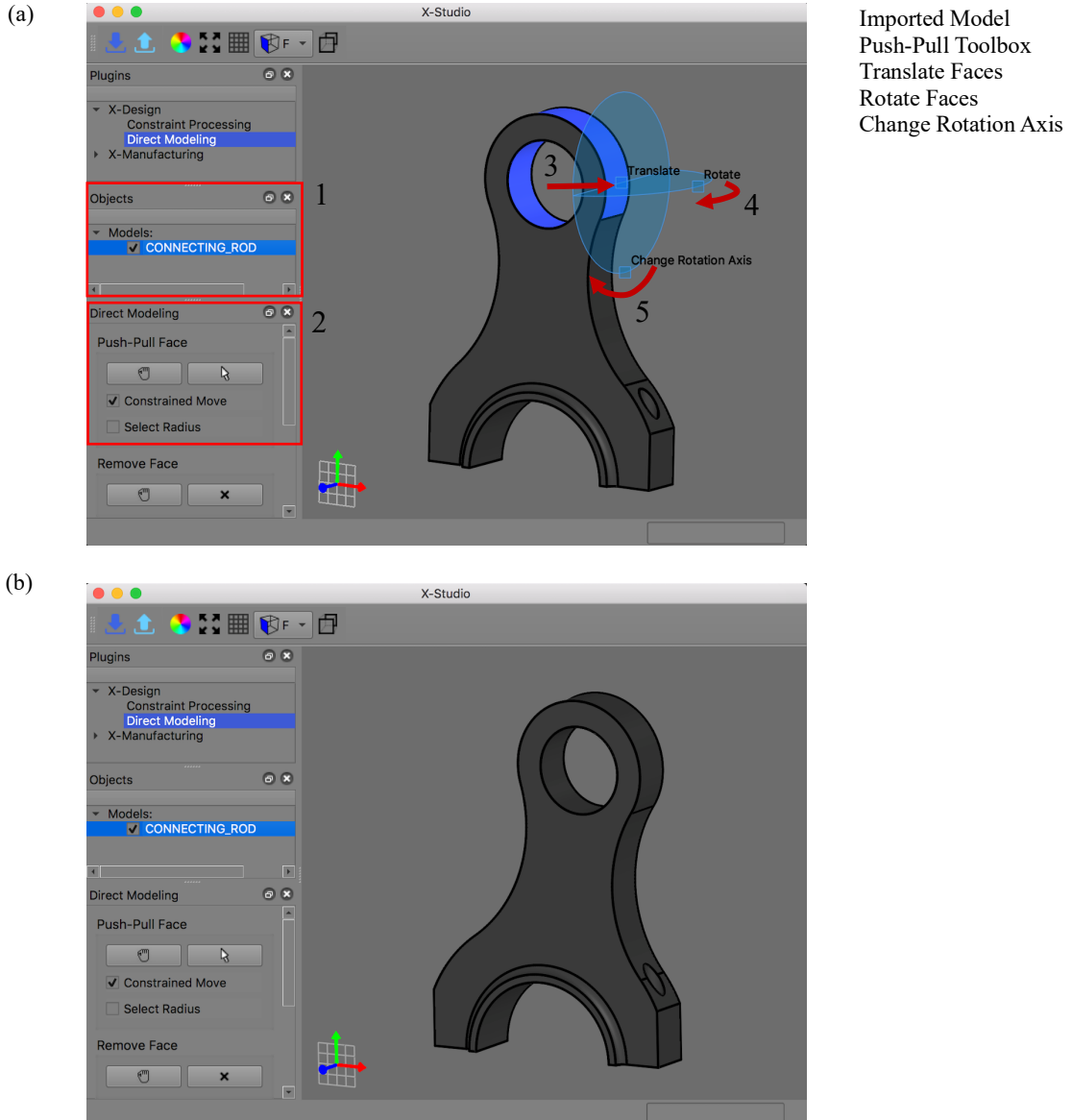


Figure 8 Graphical user interface (a) of the push-pull with  $G^1$  connection system and (b) modeling result of translating blue faces.

Push-Pull toolbox (labelled as 2 in Fig. 8a), and then selects the boundary faces of interest. Once done, a push-pull handle (labelled as 3-5 in Fig. 8a) pops up. By selecting and moving the three rectangular sub-handles in the push-pull handle, users can translate and/or rotate the selected boundary faces as they see fit. After the push-pull parameters are specified, the computer uses the methodology presented in Section 3 to carry out the model update. For instance, Fig. 8b shows the updated model for translating the blue faces by 7.5mm.

#### 4.2. Case Studies

A series of case studies have been conducted to demonstrate effectiveness of the proposed method. The modeling results were compared with those of the state of the art of commercial CAD systems. Five leading commercial CAD systems were tested: ANSYS SpaceClaim (19), Autodesk Inventor (2018), PTC Creo (Elements/Direct modeling 19), Siemens NX (11), and SolidWorks (2018). SolidWorks barely supports push-pull with  $G^1$  connections; Autodesk

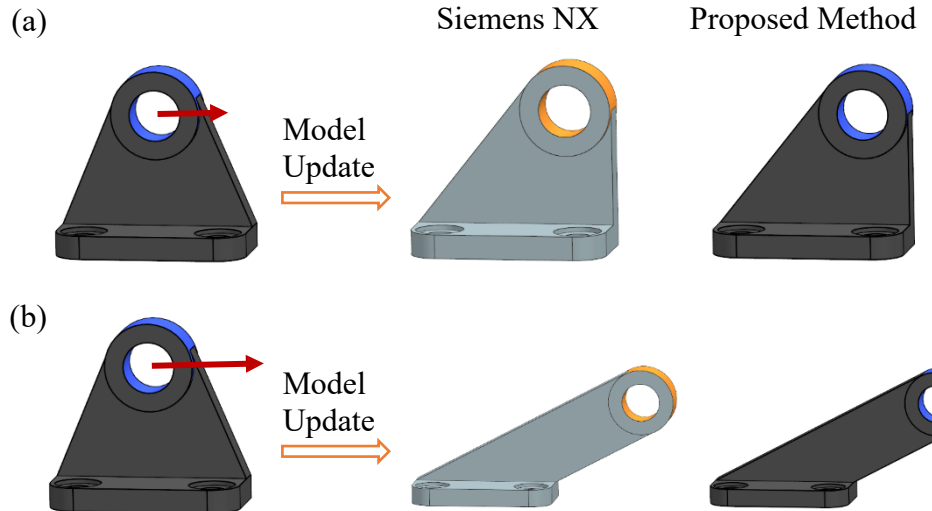


Figure 9 Push-pulling the axis support model and the modeling results: (a) a normal push-pull edit; and (b) an arbitrary push-pull edit.

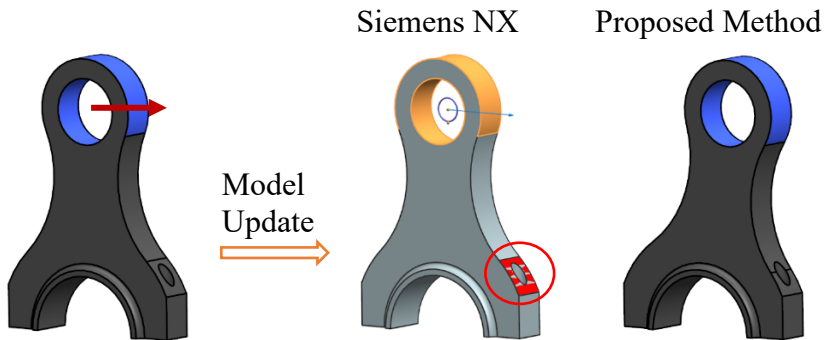


Figure 10 Push-pulling the connecting rod model and the modeling results.

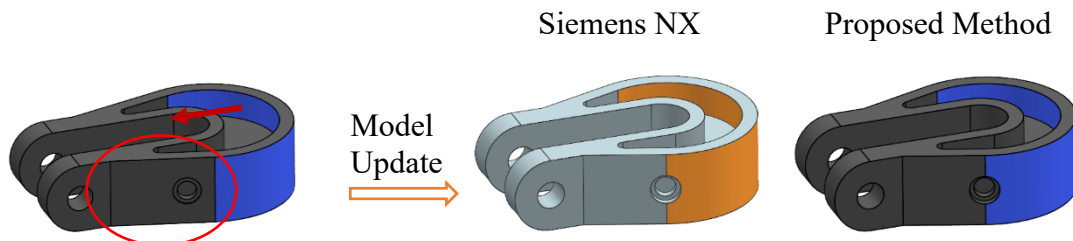


Figure 11 Push-pulling the hook model and the modeling results.

Inventor and PTC Creo partially support push-pull with  $G^1$  connections in a few selected scenarios; ANSYS SpaceClaim and Siemens NX fully support push-pull with  $G^1$  connections. Between ANSYS SpaceClaim and Siemens NX, the latter has a better performance in terms of preserving  $G^1$  connections; sometimes the former even gives distorted, nonsense model shapes. (ANSYS SpaceClaim however outperforms Siemens NX for push-pull without  $G^1$  connections.) Therefore, Siemens NX was chosen for demonstrating the comparisons.

Four mechanical parts were chosen to conduct the case studies. They were obtained from the GrabCAD part library (<https://grabcad.com/library>). Case study 1 considered push-pulling an axis support part model where no critical points

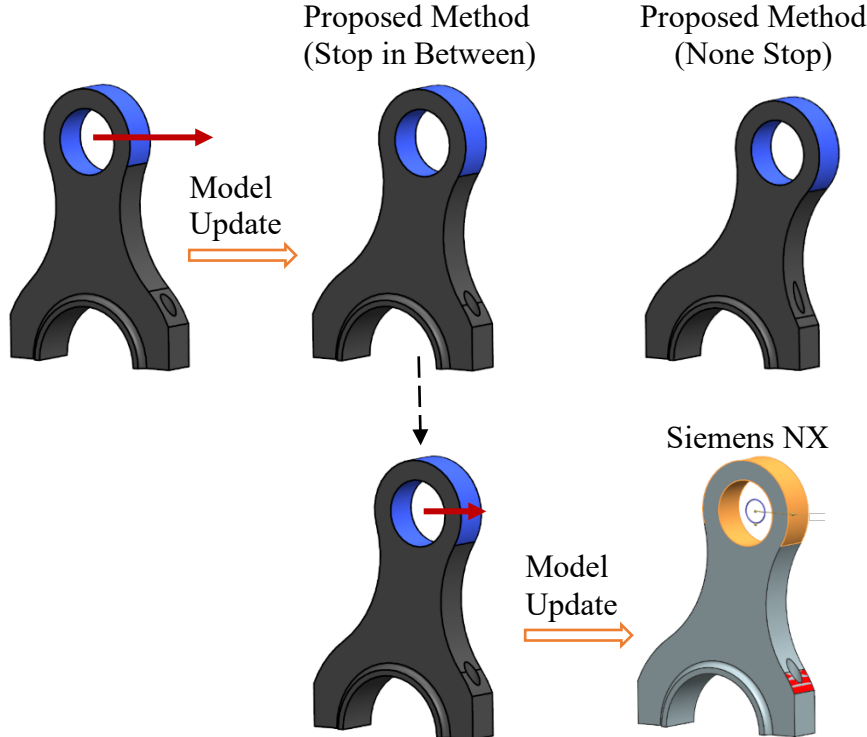


Figure 12 Revisiting case study 2.

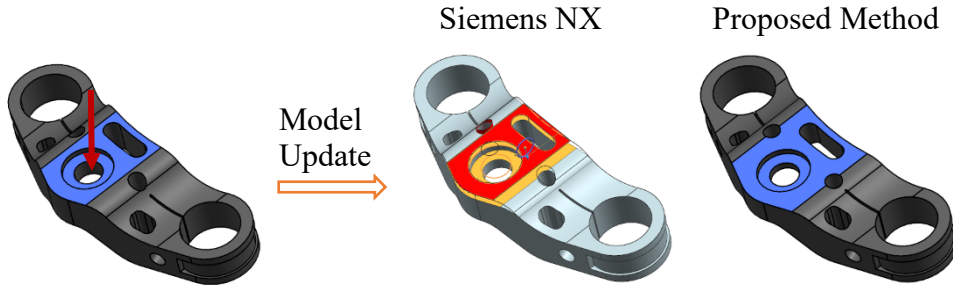


Figure 13 Push-pulling the motorcycle triple clamp model and the modeling results.

could be detected during the push-pull edit (Fig. 9). Case study 2 involved a connecting rod part model with one critical point in the push-pull edit (Fig. 10). Case study 3 analyzed push-pulling a hook part model with one critical point in the push-pull edit as well (Fig. 11). The purpose of the above three case studies is to confirm the importance of geometry-topology inconsistency detection, using the varied modeling results observed in the case studies. Case study 4 (Fig. 12) and the last case study (Fig. 13) considered two more comprehensive cases (with multiple critical points) to show effectiveness of the proposed method as a whole.

#### 4.3. Discussion

In case study 1, there was no critical point during the push-pull edit. Model update was thus made trivial and only involved model regeneration. Both Siemens NX and the proposed method successfully gave satisfactory modeling results (Fig. 9), even when the push-pull was made arbitrary (Fig. 9b). In case study 2, similar faces to those in case study 1 were push-pulled, i.e., the top cylindrical face and the face of the cylindrical hole, but an invalid modeling result was generated by Siemens NX (Fig. 10). (Siemens NX colors boundary faces in red whenever there is a model

update failure, as shown by the circled face in Fig. 10.) The only difference between case studies 1 and 2 is that the latter contains a critical point. It is thus induced that crossing critical points could cause model update failures.

Like case study 2, case study 3 involved only one critical point. What's more, the geometry-topology inconsistency and topology-changed faces are similar in both cases. That is, the regenerated boundary face for the circled face in Fig. 11 is similar to that shown in Fig. 3 (the example in Fig. 3 is same to case study 2). The two case studies are almost same in terms of the geometry-topology inconsistency configuration; however, Siemens NX failed in case study 2 and succeeded in case study 3. Thus, the failure in case study 2 was likely not due to the inconsistency resolution module. In addition, the geometric configuration is also similar in both cases, thereby excluding the failure reason of numerical instability [25]. The inconsistency detection module is thus very likely the cause. From the varied modeling results of Siemens NX in the above three case studies, an effective method for geometry-topology inconsistency detection is seen to be an essential part for attaining robust push-pull with  $G^1$  connections.

Varied modeling results were observed for Siemens NX in case studies 1-3. By contrast, the proposed method was able to robustly update the models. The push-pull edits involved in case studies 1-3 were not complex in fact, since there were at most one critical point involved. Thus, more complex cases were analyzed in the next two case studies. In case study 4, the connecting rod model was revisited (Fig. 12). The blue faces were push-pulled further to an extent that two critical points were involved. The proposed method successfully updated the model for the following three situations: (1) push-pull the blue faces and stop in between the first and second critical points (basically this is same to case study 2); (2) push-pull the blue faces, and stop in between, then continue the push-pull until the end; and (3) push-pull the blue faces until the end. The modeling result of the first situation is shown in the middle of the upper row in Fig. 12. The modeling result for the second situation is shown in the upper-right of Fig. 12. The modeling result of the third situation is same to the second one. Siemens NX failed to update the model for all of the three situations: the failure for the first situation has been shown in Fig. 10; the failure for the second situation is shown in the lower row of Fig. 12; and the third situation is clearly impossible if the first two situations are not handled successfully. Case study 5 (Fig. 13) considered a much more complex scenario where ten critical points were involved, and some of them occurred concurrently. As a result, the configuration of the geometry-topology inconsistency is complex and the associated detection task is challenging. Siemens NX was able to successfully cross the first two critical points, while the proposed method can correctly detect all the critical points and resolve the associated geometry-topology inconsistencies, as shown in Fig. 13.

## 5. Conclusions

A robust method for push-pull direct modeling while preserving  $G^1$  connections has been presented in this work. It solves the robust model update issues observed in the current commercial CAD systems. The main challenge for implementing this kind of push-pull direct modeling is the lack of the motion information of movable boundary faces and the history of the geometry-topology inconsistency caused by these movable boundary faces. This work proposes a novel method to solve this challenge. This method features the ability to detect the critical points for the geometry-topology inconsistency while avoiding the reliance on the inconsistency's history. This is the main contribution of the present work. Based on this method, it becomes possible for the existing push-pull direct modeling framework to be adapted for push-pull with  $G^1$  connections, and a robust push-pull with  $G^1$  connection method can be attained. Case studies and comparisons with the industrial state of the art have been conducted to verify the robustness of the proposed method and to show the essential role that the inconsistency detection plays in achieving robust push-pull with  $G^1$  connections.

A practical issue needs to be noted here. At first sight, the proposed reverse inference idea for geometry-topology inconsistency detection is also applicable to push-pull without  $G^1$  connections, i.e., the problems in [7,8]. Then, the whole method presented in this work can handle not only push-pull with  $G^1$  connections but also push-pull without  $G^1$  connections. However, this would lead to the “break a butterfly on a wheel” situation as motions of all movable boundary faces are known in [7,8]. More importantly, the method here is less efficient than the heuristic-based methods in [7,8] because solving systems of nonlinear equations is involved. Therefore, the proposed method, in the current form, is quite specific for push-pull with  $G^1$  connections. Improving the computational efficiency of the proposed method is among the direct modeling research studies to be carried out in our research group. In addition, combining the present work with virtual/augmented reality techniques is of great interest for future studies.

## Acknowledgements

This work has been funded in part by the Natural Sciences and Engineering Research Council of Canada (NSERC) under the Discovery Grants program.

## References

- [1] Kirkwood R, Sherwood JA. Sustained Integration for Computer-Aided Manufacturing: Integrating With Successive Versions of Step or IGES Files. *Journal of Computing and Information Science in Engineering* 2018;18:041003.
- [2] Tornincasa S, Monaco FD. The future and the evolution of CAD. *Proceedings of the 14th International Research/Expert Conference*, 2010, p. 11–8.
- [3] Ault H, Phillips A. Direct modeling: easy changes in CAD. *Proceedings of the 70th ASEE Engineering Design Graphics Division Midyear Conference*, 2016, p. 99–106.
- [4] Hashemian A, Imani BM. Surface fairness: a quality metric for aesthetic assessment of compliant automotive bodies. *Journal of Engineering Design* 2018;29:41–64.
- [5] Song H, Feng H-Y, OuYang D. Automatic Detection of Tangential Discontinuities in Point Cloud Data. *Journal of Computing and Information Science in Engineering* 2008;8:021001.
- [6] Rabbani T, Van Den Heuvel F. Efficient Hough transform for automatic detection of cylinders in point clouds. *Proceedings of the 11th Annual Conference of the Advanced School for Computing and Imaging*, 2005, p. 60–65.
- [7] Lipp M, Wonka P, Müller P. PushPull++. *ACM Transactions on Graphics* 2014;33:1–9.
- [8] Zou Q, Feng H-Y. Push-pull direct modeling of solid CAD models. *Advances in Engineering Software* 2019;127:59–69.
- [9] Li Y, Zhao W, Hu L. A Process Oriented Hybrid Resource Integration Framework for Product Variant Design. *Journal of Computing and Information Science in Engineering* 2012;12:041005.
- [10] Rossignac JR. Issues on feature-based editing and interrogation of solid models. *Computers and Graphics* 1990;14:149–72.
- [11] Woo Y, Lee SH. Volumetric modification of solid CAD models independent of design features. *Advances in Engineering Software* 2006;37:826–35.
- [12] Kim BC, Mun DW. Stepwise volume decomposition for the modification of B-rep models. *The International Journal of Advanced Manufacturing Technology* 2014;75:1393–403.
- [13] Fu J, Chen X, Gao S. Automatic synchronization of a feature model with direct editing based on cellular model. *Computer-Aided Design and Applications* 2017;14:680–92.
- [14] Shah J, Mäntylä M. *Parametric and Feature-Based CAD/CAM: Concepts, Techniques, and Applications*. John Wiley & Sons; 1995.
- [15] Hoffmann CM, Kim KJ. Towards valid parametric CAD models. *Computer-Aided Design* 2001;33:81–90.
- [16] Van der Meiden HA, Bronsvoort WF. Tracking topological changes in parametric models. *Computer Aided Geometric Design* 2010;27:281–93.
- [17] Hidalgo M, Joan-Arinyo R. Computing parameter ranges in constructive geometric constraint solving: implementation and correctness proof. *Computer-Aided Design* 2012;44:709–20.
- [18] Requicha AAG. Representations for rigid solids: theory, methods, and systems. *ACM Computing Surveys* 1980;12:437–64.
- [19] Bondy JA, Murty USR. *Graph Theory with Applications*. Graph Theory 1976;290:270.
- [20] Braid IC. Geometric modelling. *Advances in Computer Graphics I*, Springer; 1986, p. 325–62.
- [21] Do Carmo MP. *Differential Geometry of Curves and Surfaces*. Prentice Hall; 1976.
- [22] Bettig B, Shah J. Derivation of a standard set of geometric constraints for parametric modeling and data exchange. *Computer-Aided Design* 2001;33:17–33.
- [23] Raghothama S, Shapiro V. Boundary representation deformation in parametric solid modeling. *ACM Transactions on Graphics* 1998;17:259–86.
- [24] Möbius J, Kobbelt L. OpenFlipper: an open source geometry processing and rendering framework. *Proceedings of the International Conference on Curves and Surfaces*, 2012, p. 488–500.
- [25] Hoffmann CM. Robustness in Geometric Computations. *Journal of Computing and Information Science in Engineering* 2001;1:143–55.